

Low-pump sum frequency generation of frequency-stabilized 453 nm blue laser for photonic quantum interface

Jian Wang (王健)^{1,2}, Yuhao Pan (潘宇豪)^{1,2}, Yunfeng Huang (黄运锋)^{1,2,*},
Chuanfeng Li (李传锋)^{1,2}, and Guangcan Guo (郭光灿)^{1,2}

¹CAS Key Laboratory of Quantum Information, University of Science and Technology of China,
Hefei 230026, China

²Synergetic Innovation Centre in Quantum Information and Quantum Physics, University of Science and
Technology of China, Hefei 230026, China

*Corresponding author: hyf@ustc.edu.cn

Received September 30, 2017; accepted October 13, 2017; posted online November 9, 2017

Generation of a cavity-enhanced nondegenerate narrow-band photon pair source is a potential way to realize a perfect photonic quantum interface for a hybrid quantum network. However, to ensure the high quality of the photon source, the pump laser for the narrow-band photon source should be generated in a special way. Here, we experimentally generate the blue 453 nm laser with a sum frequency generation process in a periodically poled lithium niobate waveguide. A 13 mW laser at 453 nm can be achieved with a low-power 880 nm laser and 935 nm laser input, and the internal conversion efficiency is 21.6% after calculation. The frequency of a 453 nm laser is stabilized by locking two pump lasers on one ultrastable optical cavity. The single pass process without employing cavity enhancement can ensure a good robustness of the whole system.

OCIS codes: 270.5585, 140.3613, 190.7220.

doi: 10.3788/COL201715.122701.

The building of a quantum network is of great importance for the development of quantum communication and distributed quantum computation^[1]. However, owing to the inherent defects of single physical systems, a quantum network with single physical systems cannot take its roles described above efficiently. The universal form of a quantum network, a hybrid quantum network consisting of various physical systems, has been proposed^[2] and developed to avoid these limitations^[3-5]. The main obstacle standing in the way is the realization of the photonic quantum interface compatible with the quantum nodes in the hybrid quantum network^[2]. To realize this kind of photonic quantum interface, one potential proposal is to use a cavity-enhanced nondegenerate narrow-band photon pair source^[6].

Since the first cavity-enhanced narrow-band photon pair source was proposed and experimentally generated, lots of relative work in this area have been developed^[10-15] and used for quantum communication and quantum metrology^[16,17]. The generated photons matched with the cavity modes can be enhanced greatly, otherwise, suppressed greatly. For the needs of interfacing the quantum nodes, the central wavelength and bandwidth of the generated photon should be matched precisely with the quantum nodes. This gives special demands on the strategy of the generation of a pump laser for the photonic quantum interface, which means that the pump laser should be generated with the double frequency or sum frequency with the same lasers matched with the quantum nodes.

In our case, we try to realize the photonic quantum interface for the trapped ion Yb⁺ (working wavelength of 935 nm) and rare-earth-doped solid state quantum memory (working wavelength of 880 nm)^[18]. So, a 453 nm pump laser satisfies all of the needs above that should be generated in the experiment. The nonlinear optical process is a widely used method to get different kinds of laser beams^[19-21]. For this case, the common way to get the pump laser is by employing the cavity-enhancement effect to get a large conversion efficiency^[22-26]. With a nonlinear crystal inserted into a bow-tie cavity and some necessary active locking processes, the pump laser with sum frequency generation (SFG) can be obtained efficiently. However, the strategy of active locking easily suffers from the disturbance of the environment and decreases the stability of the whole system. The nonlinear process of a periodically poled lithium niobate (PPLN) waveguide is another method to obtain the pump laser^[27-29]. Benefiting from its high optical power density due to the tight confinement of photons in the structure of the waveguide, the single pass conversion efficiency will be high enough for the SFG process.

Here, we used the SFG process in the PPLN waveguide to obtain a 453 nm blue pump laser. The single pass SFG process ensures high stability of this pump laser. The internal conversion efficiency of the nonlinear process is 21.6% with the low-power laser's input. The frequency of the generated blue laser is stabilized by locking the frequencies of input lasers on the same ultrastable optical cavity (UOC).

The experimental setup of the SFG of the 453 nm blue laser is shown in Fig. 1. It mainly consists of two parts: the laser frequency stabilization part and the SFG in the PPLN waveguide part. In the laser frequency stabilization part, two semiconductor external cavity-diode lasers with target wavelengths at 880 nm (Moglabs) and 935 nm (Toptica DL pro) are locked to the same ultrastable Fabry–Pérot (FP) cavity with a 1 MHz bandwidth and 1500 finesse (Stable Laser Systems) with the Pound–Drever–Hall (PDH) scheme^[30]. The ultrastable FP cavity is placed in a high vacuum chamber and temperature-controlled with the precision of 10 mK, which can ensure the ultrastable FP cavity as an ideal frequency reference. The polarization beam splitter (PBS) and quarter-wave plate (QWP) are the standard modules usually used to realize the PDH laser frequency stabilization. Photodiodes (PDs) are used to detect the reflected optical signals and then demodulated to the error signals. In the SFG in the PPLN waveguide part, its main module is a 1-cm-long periodically poled MgO-doped LiNbO₃ ridge waveguide (PPLN waveguide, the size is 10 mm × 1.5 mm × 0.5 mm provided by HCPhotonics Corp). The chip of the waveguide is sealed in the module, and it is temperature-controlled with the precision of 0.1 K to ensure the quasi-phase-matching condition, which is one of the phase-matching methods and can ensure conservation of the momentum in the nonlinear optical process^[31]. In this case, the phase-matching condition is

$$\Delta k(t) = k_{880}(t) + k_{935}(t) - k_{453}(t) - k_m(t), \quad (1)$$

where $k_{880}(t)$, $k_{935}(t)$, and $k_{453}(t)$ are the wave vectors of the 880 and 935 nm input lasers and the 453 nm output laser. $k_m(t)$ is the optical grating wave vector caused by the periodically poled structure. $\Delta k(t)$ is the phase mismatching of the nonlinear process. All of these parameters can be varied with the temperature of the

nonlinear crystal. In the experiment, to obtain the best conversion efficiency, the nonlinear crystal should be temperature-controlled to realize the phase-matching condition [$\Delta k(t) = 0$]^[28]. The input and output facets of the waveguide is anti-reflecting coated for 880, 935, and 453 nm wavelengths ($R < 0.5\%$), which ensure that the 880 and 935 nm lasers transmit the waveguide only once, and the generated 453 nm blue laser is emitted efficiently. In the input port of the waveguide, a polarization-maintained fiber (PMF) pigtail is integrated to get a relatively robust interface, its directions of optical axes are precisely matched with the directions of optical axes of the PPLN waveguide, and the polarization of the input laser is rotated by the half-wave plate (HWP) inserted before the fiber coupler (FC), which can ensure that the input laser take part in the SFG efficiently. Besides, two lens assemblies are independently used to realize the efficient laser–fiber coupling (80% for the 935 nm laser, 75% for the 880 nm laser). In the output port, to get much more fiber-collecting efficiency and match the strategy of the generated narrow-band photon source, it has to be a free space output.

To better explore the potential of the PPLN waveguide, we first measure the critical phase-matching temperature. Especially for SFG, its real value has a big deviation with the theoretically calculated value. After checking that the polarization of the output pump lasers are well aligned with the optical axes of the PPLN waveguide, the power of the generated 453 nm blue laser will change with the tuning of the temperature of the waveguide, depending on the phase-matching condition. The data is shown in Fig. 2. The highest power of the generated 453 nm blue laser is obtained when the temperature of the waveguide is tuned to 60.4°C, which is much different with the inferred value of 36.1°C (provided by HCPhotonics Corp). According to the nonlinear optics theory^[32], the power of the SFG 453 nm laser can be expressed as follows:

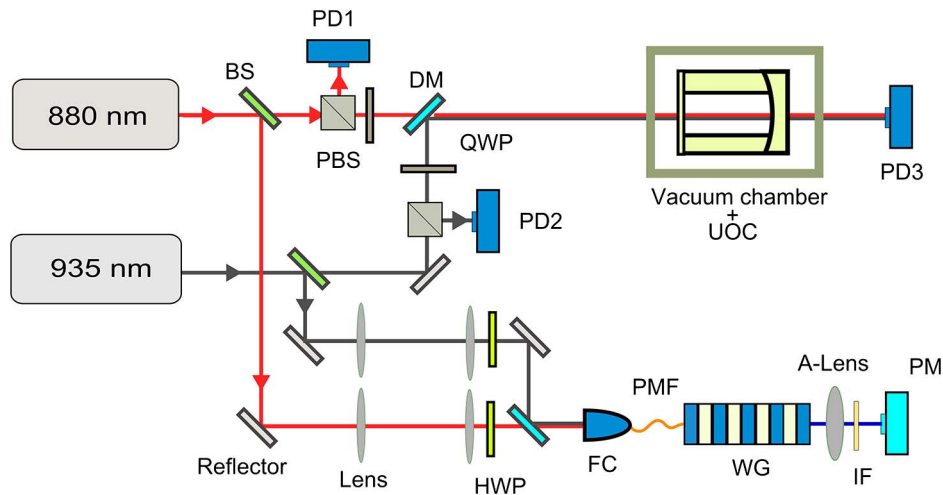


Fig. 1. (Color online) Experimental setup. BS, beam splitter; DM, dichroic mirror; IF, interference filter; A-lens, aspheric lens; PM, power meter; WG, waveguide. The red line represents the 880 nm laser, the gray line represents the 935 nm laser, and the blue line represents the 453 nm pump laser. DMs are used here to combine the 935 nm laser and the 880 nm laser together.

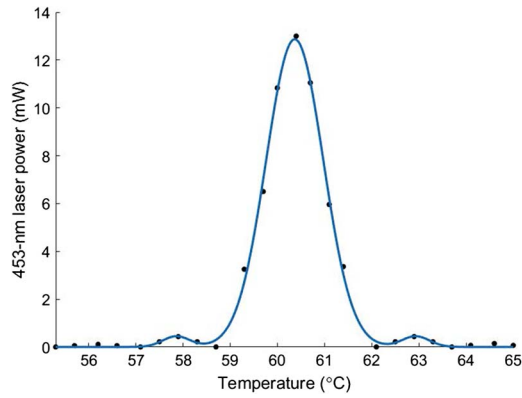


Fig. 2. Relation between the 453 nm laser output and the temperature of the PPLN waveguide.

$$P_{453} \propto P_{935} P_{880} L^2 d_{\text{eff}}^2 \text{sinc}^2(\Delta k L / 2), \quad (2)$$

where P_{453} , P_{935} , and P_{880} are the powers of the 453 nm blue laser, 880 nm laser, and 935 nm laser, separately. L is the length of the PPLN waveguide. d_{eff} is the effective nonlinear coefficient. Using this equation to fit the data in Fig. 2, the full width at half-maximum (FWHM) of the phase-matching temperature can be inferred to be 1.4°C, which implies that the temperature-controlled precision of 0.1 K should be good enough to get a relatively stable output. The stability of the output laser will be shown later.

The SFG process depends on the powers of the input lasers. So, the power and conversion efficiency are measured to further explore the potential of the nonlinear process in the experiment. Notably, we take the process that the power of the 453 nm laser generated by changing the input power of the 935 nm laser, for example. The output power and conversion efficiency are shown in Figs. 3 and 4, independently. It shows a linear relation between the output power and the power of the input 935 nm laser in the region that the diode laser can provide, which is fitted quite well according to the description of Eq. (2).

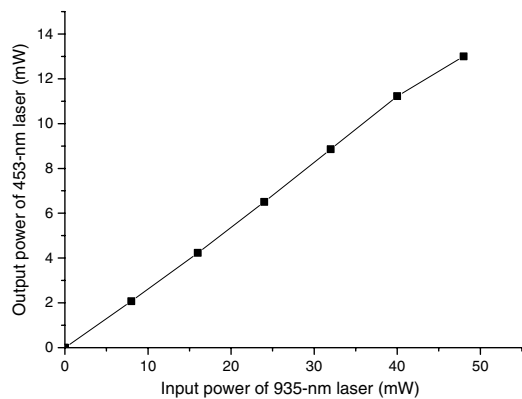


Fig. 3. Relation between the output power of the generated 453 nm laser with input power of the 935 nm laser. Here, the input power of the 880 nm laser is 12 mW, and the biggest power of the 935 nm laser is 48 mW.

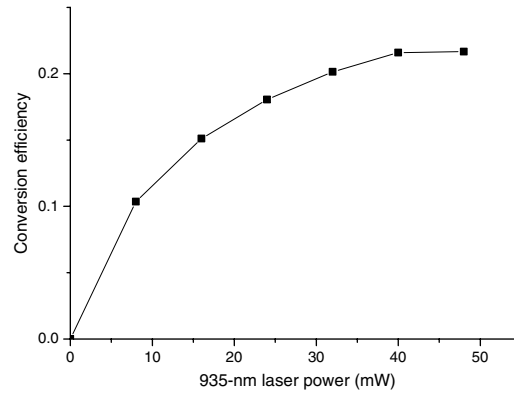


Fig. 4. Relation between the conversion efficiency and the input power of the 935 nm laser.

The highest generated power of the 453 nm blue laser is 13 mW. For the conversion efficiency, the highest value is 21.6% at the situation of the highest 935 nm laser input, which is inferred by $P_{453}/(P_{880} + P_{935})$. Considering the quite low powers of the pump laser, this conversion efficiency is comparable with some previous works^[27–29]. The increasing trend of the conversion efficiency shows that the pump power will reach the saturated area^[33]. Besides, the data of the powers of the input lasers are the actual values inside the waveguide.

The long-term stability of the 453 nm blue laser output power is also measured, which is shown in Fig. 5. It mainly shows that the laser output power changes with the actual measurement time at the situation of maximum output. The overall measurement time is 1 h with the time interval of 10 min. It turns out that the fluctuation of the output laser power is 1% without any feedback power control. The main cause of this problem is the temperature changes that resulted from the environment and blue photon absorption by the waveguide. In fact, some additional measures are taken to get a relatively stable output power, including isolating the waveguide from the environment with a homemade shield.

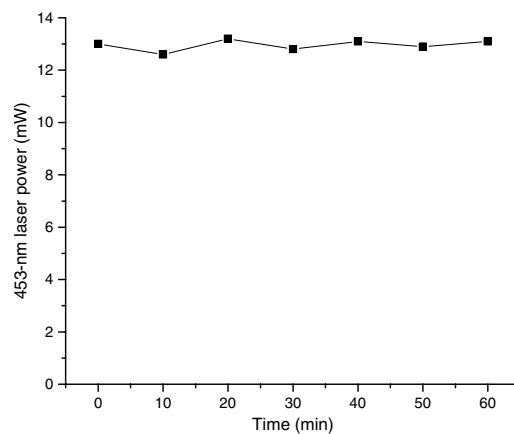


Fig. 5. Measurement of the long-term stability of the generated blue laser.

For a good photonic interface, the central frequencies of the photons should be perfectly matched with the atomic absorption spectrometry line, which requires that the central frequency of the blue pump laser should be locked to some reference standards. In this case, owing to the SFG of the 453 nm blue laser, the best way to stabilize the frequency of the blue laser is by locking the frequencies of the input 880 and 935 nm lasers. The locking scheme here is the widely used PDH method, which is insensitive to the power fluctuation and robust to the environmental disturbance^[30]. Owing to the ultrastable FP cavity and lasers, the perfect transmission signal and error signal can be achieved in the experiments, which result in good locking of the frequencies of the lasers. Considering the linewidth of the FP cavity is 1 MHz, we can conservatively infer that the stability of the laser frequency is less than 500 kHz, which is much better for the demand of a photonic interface.

In conclusion, we use the SFG process in the PPLN waveguide to obtain a 453 nm blue pump laser, which can be used for the photonic interface. The single pass process without employing cavity enhancement can ensure a good robustness of the whole system. With a 12 mW 935 nm laser input and a 48 mW 880 nm laser input, we can obtain a 13 mW 453 nm blue laser output, and the internal conversion efficiency of nonlinear process is 21.6%, which is comparable with previous works. Besides, the frequency of the generated blue laser is also stabilized by locking the frequencies of input lasers on the reference standards. Our work provides a robust way to generate the frequency-stabilized 453 nm blue laser with low-power pump lasers that are compatible with the photonic interface, which will be useful for the development of the hybrid quantum network.

This work was supported by the National Key Research and Development Program of China (No. 2017YFA0304100), the National Natural Science Foundation of China (Nos. 61327901, 11325419, and 11474268), the Key Research Program of Frontier Sciences, CAS (No. QYZDY-SSW-SLH003), the National Program for Support of Topnotch Young Professionals (No. BB2470000005), and the Fundamental Research Funds for the Central Universities (Nos. WK2470000026 and WK2470000018).

References

1. J. Kimble, *Nature* (London) **453**, 1023 (2008).
2. M. Wallquist, K. Hammerer, P. Rabl, M. Lukin, and P. Zoller, *Phys. Scr.* **T137**, 014001 (2009).
3. H. M. Meyer, R. Stockill, M. Steiner, C. Le Gall, C. Matthiesen, E. Clarke, A. Ludwig, J. Reichel, M. Atatüre, and M. Köhl, *Phys. Rev. Lett.* **114**, 123001 (2015).
4. J.-S. Tang, Z.-Q. Zhou, Y.-T. Wang, Y.-L. Li, X. Liu, Y.-L. Hua, Y. Zou, S. Wang, D.-Y. He, G. Chen, Y.-N. Sun, Y. Yu, M.-F. Li, G.-W. Zha, H.-Q. Ni, Z.-C. Niu, C.-F. Li, and G.-C. Guo, *Nat. Commun.* **6**, 8652 (2015).
5. Z.-L. Xiang, S. Ashhab, J. Q. You, and F. Nori, *Rev. Mod. Phys.* **85**, 623 (2013).
6. G. Kurizkia, P. Bertet, Y. Kubob, K. Molmer, D. Petrosyan, P. Rabl, and J. Schmiedmayer, *Proc. Natl. Acad. Sci. USA* **112**, 3866 (2014).
7. S. Kotler, R. W. Simmonds, D. Leibfried, and D. J. Wineland, *Phys. Rev. A* **95**, 022327 (2017).
8. R. Zhao and R. Liang, *Chin. Opt. Lett.* **14**, 062701 (2016).
9. C. Simon, H. de Riedmatten, M. Afzelius, N. Sangouard, H. Zbinden, and N. Gisin, *Phys. Rev. Lett.* **98**, 190503 (2007).
10. Z.-Y. Ou and Y.-J. Lu, *Phys. Rev. Lett.* **83**, 2556 (1999).
11. C. E. Kuklewicz, F. N. C. Wong, and J. H. Shapiro, *Phys. Rev. Lett.* **97**, 223601 (2006).
12. X.-H. Bao, Y. Qian, J. Yang, H. Zhang, Z.-B. Chen, T. Yang, and J.-W. Pan, *Phys. Rev. Lett.* **101**, 190501 (2008).
13. M. Scholz, L. Koch, and O. Benson, *Phys. Rev. Lett.* **102**, 063603 (2009).
14. F. Wolfgramm, Y. A. de Icaza Astiz, F. A. Beduini, A. Cerè, and M. W. Mitchell, *Phys. Rev. Lett.* **106**, 053602 (2011).
15. J. Fekete, D. Rieländer, M. Cristiani, and H. de Riedmatten, *Phys. Rev. Lett.* **110**, 220502 (2013).
16. H. Zhang, X.-M. Jin, J. Yang, H.-N. Dai, S.-J. Yang, T.-M. Zhao, J. Rui, Y. He, X. Jiang, F. Yang, G.-S. Pan, Z.-S. Yuan, Y.-J. Deng, Z.-B. Chen, X.-H. Bao, and S. Chen, B. Zhao and J.-W. Pan, *Nat. Photon.* **5**, 628 (2011).
17. D. Rieländer, K. Kutluer, P. M. Ledingham, M. Gündoğan, J. Fekete, M. Mazzer, and H. de Riedmatten, *Phys. Rev. Lett.* **112**, 040504 (2014).
18. J. Wang, P.-Y. J. Lv, J.-M. Cui, B.-H. Liu, J.-S. Tang, Y.-F. Huang, C.-F. Li, and G.-C. Guo, *Phys. Rev. Appl.* **4**, 064011 (2015).
19. J.-Y. Zhao, I. D. Chremmos, Z. Zhang, Y. Hu, D.-H. Song, P. Zhang, N. K. Efremidis, and Z.-G. Chen, *Sci. Bull.* **60**, 1157 (2015).
20. A. Shapira, L. Naor, and A. Arie, *Sci. Bull.* **60**, 1403 (2015).
21. R. Cao, B. Gai, J. Yang, T. Liu, J. Liu, S. Hu, J. Guo, Y. Tan, S. He, W. Liu, H. Cai, and X. Zhang, *Chin. Opt. Lett.* **13**, 121903 (2015).
22. Y. Lu, X. Zhang, and Z. Yao, *Chin. Opt. Lett.* **5**, 353 (2007).
23. Y. Yu, G. Jin, C. Wang, X. Chen, J. Guo, and Y. Wang, *Chin. Opt. Lett.* **34**, 1024 (2009).
24. Y. Lv, H. Tan, and L. Qian, *Chin. Opt. Lett.* **4**, 25 (2006).
25. X. Chen, X. Li, H. Zhang, H. Chen, J. Bai, and Z. Ren, *Chin. Opt. Lett.* **7**, 815 (2009).
26. Y. Shang, M. Shen, P. Wang, X. Li, and X. Xu, *Chin. Opt. Lett.* **14**, 121901 (2016).
27. T. Nishikawa, A. Ozawa, Y. Nishida, M. Asobe, F.-L. Hong, and T. W. Hänsch, *Opt. Express* **17**, 17792 (2009).
28. J. Wang, J.-Q. Sun, C.-H. Luo, and Q.-Z. Sun, *Opt. Express*, **13**, 7405 (2005).
29. L.-N. Zhao, J. Su, X.-P. Hu, X.-J. Lv, Z.-D. Xie, G. Zhao, P. Xu, and S.-N. Zhu, *Opt. Express* **18**, 13331 (2010).
30. E. D. Black, *Am. J. Phys.* **69**, 79 (2001).
31. V. Pasiskevicius, G. Strömquist, F. Laurell, and C. Canaliase, *Opt. Mater.* **34**, 513 (2012).
32. R. W. Boyd, *Nonlinear Optics*, 2nd ed. (Academic, 2003).
33. B. Albrecht, P. Farrera, X. Fernandez-Gonzalvo, M. Cristiani, and H. de Riedmatten, *Nat. Commun.* **5**, 3376 (2014).